OPTIMAL CONTROL APPLICATIONS AND METHODS
Optim. Control Appl. Meth. 2008; **29**:257–277
Published online 3 September 2007 in Wiley InterScience (www.interscience.wiley.com). DOI: 10.1002/oca.820

Time-optimal control of flexible systems subject to friction

Jae-Jun Kim[‡], Rajaey Kased[§] and Tarunraj Singh[*, †, ¶]

Department of Mechanical and Aerospace Engineering, State University of New York at Buffalo, Buffalo, New York, NY 14260, U.S.A.

SUMMARY

This paper presents a technique for the determination of time-optimal control profiles for rest-to-rest maneuvers of a mass–spring system, subject to Coulomb friction. A parameterization of the control input that accounts for the friction force, resulting in a linear analysis of the system is proposed. The optimality condition is examined for the control profile resulting from the parameter optimization problem. The development is illustrated on a single input system where the control input and the friction force act on the same body. The variation of the optimal control structure as a function of final displacement is also exemplified on the friction benchmark problem. Copyright © 2007 John Wiley & Sons, Ltd.

Received 18 May 2005; Revised 3 April 2007; Accepted 18 July 2007

KEY WORDS: time-optimal control; friction; time-delay filter; input shaping

1. INTRODUCTION

Mechanical systems involving relative motion are always under the influence of frictional forces. Therefore, it is important to include the frictional effect for designing controllers when precise regulation of the system is required. However, the friction phenomenon involves very complex processes such as pre-sliding, local memory, and frictional lag [1]. Since the friction force is highly nonlinear in the small velocity region, flexible systems with vibratory motion may cause stick–slip. Therefore, finding a time-optimal controller for such a system is a challenging problem.

The problem of designing a time-optimal control in the presence of structural flexibility has been well studied especially for flexible spacecraft [2]. Most often, the modelling of the system relies on the assumed mode method in conjunction with the Euler–Bernoulli beam theory, and

*Correspondence to: Tarunraj Singh, Department of Mechanical and Aerospace Engineering, SUNY at Buffalo, Buffalo, New York, NY 14260, U.S.A.
†E-mail: tsingh@eng.buffalo.edu
‡NRC Research Associate, Naval Postgraduate School.
§Graduate Student.
¶Professor.

the resulting system can be modelled as a decoupled set of equations of rigid body modes and flexible modes. The time-optimal controller design with this model can be found in numerous papers [3–6].

Input shaping is a technique to eliminate vibration of a system by pre-shaping the control input to cancel the flexible dynamics of the system. Input shaping is developed for practical applications in [7], where a sequence of impulses is introduced to shape the control input. Since then, input shaping has been successfully adopted for many vibration control problems including time-optimal saturating controllers for flexible structures [4, 5]. Singh and Vadali proposed a frequency domain technique to parameterize the time-optimal control profile using a time-delay filter which shapes the step input into a bang-bang control input [6]. For time-optimal design, the time-delay filter is synthesized to cancel all the poles of the system while satisfying the state boundary conditions. The time-delay filter approach is especially effective for designing saturating controllers such as robust time-optimal, fuel-time optimal, minimum power/jerk, and jerk limited time-optimal controllers [6, 8–10]. A tutorial on input shaping and time-delay filters can be found in [11].

The input shaping and time-delay filter techniques require the system to be linear. There have been some efforts to come up with a time-optimal design for frictional system. Kim and Ha [12] used a phase-plane approach for the time-optimal design of single degree of freedom mechanical systems with friction. The resulting control has a closed-form solution but the analysis is limited to second-order systems. Driessen and Sadegh [13] formulated a mixed integer linear programming problem to design a near time-optimal controller including the Coulomb friction effect. Since the signum function is restricted to values of 1 or -1, the velocity-dependent Coulomb friction force can be represented by a binary variable. However, finding an accurate optimal control profile with the mixed integer programming problem is computationally very expensive, and the accuracy is limited by the number of samples and the convergence tolerance. Recently, the input shaping technique has been applied to a second-order system under the influence of Coulomb friction [14].

In this paper, the time-optimal control of the single input flexible system is developed where the actuated mass is also subject to Coulomb friction. The proposed development illustrates that the time-delay filter can be used to determine the optimal control profile for certain maneuvers. This is possible by parameterizing an equivalent input that includes the Coulomb friction effect. A new technique to solve for the switch and the final times is also presented for certain maneuvers where the time-delay filter cannot be used. These techniques will result in a problem of finding an optimal set of switching parameters of a control input. These parameter optimization techniques for the design of time-optimal controllers are well addressed in earlier research [15–17]. For verification of the optimality, the necessary condition for optimality is also included for the proposed techniques. The numerical simulation is performed on a two-mass benchmark problem, where the Coulomb friction is acting on the first mass. The resulting controller can be applied to many applications such as hard disk drives and flexible robot arms, where the friction force is acting on the pivot and the position at the end of the flexible structure needs to be regulated.

2. PROBLEM FORMULATION

Figure 1 illustrates a general p mass–spring system. A single control input acts on the the sth mass, which is also subject to the Coulomb friction f_c. The time-optimal problem statement for

DOI: 10.1002/oca

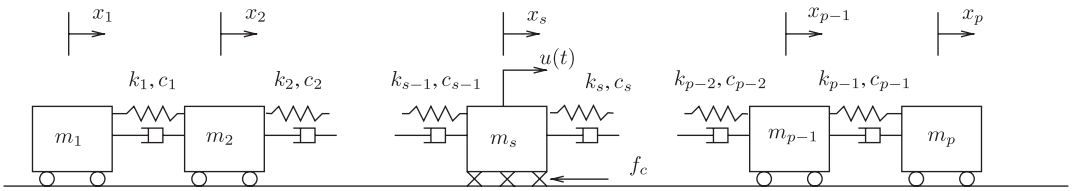

Figure 1. General p mass–spring system subject to friction.

a rest-to-rest maneuver is given as

$$\begin{aligned} \min \quad & \int_0^{t_f} \mathrm{d}t \\ \text{s.t.} \quad & \dot{\underline{x}}(t) = A\underline{x}(t) + B(u(t) - f_c \ \mathrm{sign}(\dot{x}_s)) \\ & \underline{x}(0) = \underline{x}_0, \quad \underline{x}(t_f) = \underline{x}_f \\ & -U \leqslant u(t) \leqslant U \end{aligned} \tag{1}$$

where A and B are defined as

$$A = \begin{bmatrix} 0_{p\times p} & I_{p\times p} \\ -M^{-1}K & -M^{-1}C \end{bmatrix}, \quad B = \begin{bmatrix} 0_{p\times 1} \\ M^{-1}D \end{bmatrix} \tag{2}$$

M, K, and C are the mass, stiffness, and damping matrices, respectively. D is a control influence vector of zeros with a nonzero value in the sth entry. f_c is the Coulomb friction force that is assumed to be constant. The Hamiltonian is defined as

$$\mathbf{H}(\underline{x}, \underline{\lambda}, u, t) = 1 + \underline{\lambda}^{\mathrm{T}}(A\underline{x}(t) + B(u(t) - f_c \ \mathrm{sign}(\dot{x}_s))) \tag{3}$$

and the resulting necessary conditions for optimality are given as

$$\dot{\underline{x}}(t) = \frac{\partial \mathbf{H}}{\partial \underline{\lambda}(t)} \tag{4}$$

$$\dot{\underline{\lambda}}(t) = -\frac{\partial \mathbf{H}}{\partial \underline{x}(t)} \tag{5}$$

From Pontryagin's Maximum Principle, the controller that minimizes the Hamiltonian is

$$u = -U \ \mathrm{sign}(B^{\mathrm{T}}\underline{\lambda}(t)) \tag{6}$$

where $B^{\mathrm{T}}\underline{\lambda}(t)$ is the switching function. Therefore, the time-optimal solution for this system is a bang-bang profile. However, if stiction occurs during the maneuver, the friction force becomes a function of the states and input to the system, which will be discussed in a later section.

DOI: 10.1002/oca

3. PARAMETERIZATION OF CONTROL

It has been previously shown by Singh and Vadali [6] that time-delay filters can be used to cancel the flexible dynamics of a linear system during a rest-to-rest maneuver. The well-known bang-bang control for time-optimal problems is parameterized by the unknown switching and final times, and parameter optimization is performed to determine these unknowns. Since Coulomb friction model exhibits hard nonlinearity near zero velocity, the time-delay filter approach cannot be used in its current form. In order to apply the time-delay filter technique to frictional systems, a linearizing net input is defined as

$$u_{\text{net}}(t) = u(t) - f_c \ \text{sign}(\dot{x}_s) \tag{7}$$

Since the nonlinearity of the system is taken into account with this net input, the system to be analyzed becomes linear. Then, the system equation shown in Equation (1) can be re-written in the linear form as

$$\dot{\underline{x}}(t) = A\underline{x}(t) + Bu_{\text{net}}(t) \tag{8}$$

If we parameterize the net input, $u_{\text{net}}(t)$, instead of the actual input, $u(t)$, then the time-delay filters can be used to solve the time-optimal problem stated in Equation (1). In order to solve the time-optimal problem, the net input is parameterized to form a time-delay filter, where the zeros of the time-delay filter should cancel the rigid and flexible body poles of the system as well as satisfy the boundary conditions of the problem. In addition, since the net input is parameterized instead of the actual input, there will be added constraints such that the velocity must be zero at the time when the friction term changes sign. Figure 2 shows a schematic of developing a linearizing net input for an illustrative two-mass–spring system, where the control and frictional forces act on the first mass. The velocity profile of the first mass is assumed to be of the form illustrated in the first plot in Figure 2. The actual input to the system is assumed to be three switch bang-bang as shown in the second plot in Figure 2. From the assumed velocity profile, the friction force can be determined because the friction is only a function of velocity without stiction. Then the net input is determined as the final plot, which is the sum of actual input and friction force.

For the general multiple mass–spring system shown in Figure 1, we assume that the control has n switch times at the ℓ_ith time instants ($i = 1 \ldots n$) and the velocity of the sth mass is assumed to change its sign m times at the k_jth time instants ($j = 1 \ldots m$). For example, $\ell = [1, 3, 5]$ ($n = 3$) and $k = [2, 4]$ ($m = 2$) for the problem in Figure 2. The time-delay filter that generates the control profile when driven by a unit step input can be parameterized as

$$G(s) = (U - f_c) + 2U \sum_{i=1}^{n} (-1)^i \mathrm{e}^{-sT_{\ell_i}} + 2f_c \sum_{j=1}^{m} (-1)^{j+1} \mathrm{e}^{-sT_{k_j}} + (U + f_c)\mathrm{e}^{-st_f} \tag{9}$$

$G(s)$ must cancel out all the poles of the system while the control input satisfies the final boundary conditions given in Equation (1). One of the rigid body poles is cancelled due to Equation (9) having a zero at $s = 0$. To cancel the other rigid body pole, the ~~time~~ derivative of Equation (9) must also have a zero at $s = 0$. This satisfies the velocity boundary condition for a rest-to-rest maneuver, which will yield the following constraint:

$$\left.\frac{\mathrm{d}G(s)}{\mathrm{d}s}\right|_{s=0} = -2U \sum_{i=1}^{n} (-1)^i T_{\ell_i} - 2f_c \sum_{j=1}^{m} (-1)^{j+1} T_{k_j} - (U + f_c)t_f = 0 \tag{10}$$

DOI: 10.1002/oca

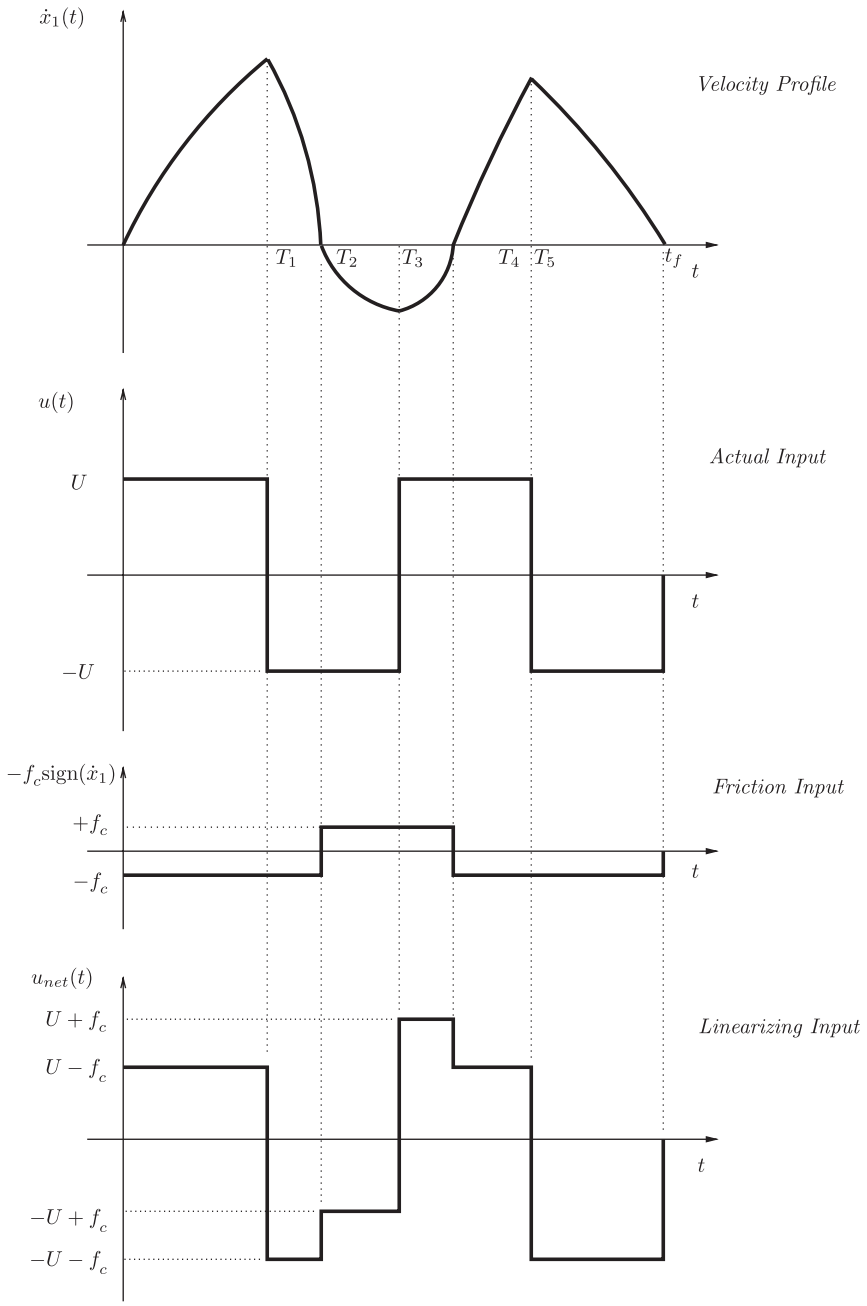

Figure 2. Schematic of linearizing input parameterizations for a two-mass–spring system.

DOI: 10.1002/oca

The filter must also cancel out the flexible mode poles, which will lead to the next $(2p-2)$ constraints. Substituting $s_\mu = \sigma_\mu + \mathrm{i}\omega_\mu$ into Equation (9) yields the following equations:

$$0 = (U - f_c) + (U + f_c)\mathrm{e}^{-t_f\sigma_\mu}\cos(t_f\omega_\mu) + 2U\sum_{i=1}^{n}(-1)^i\mathrm{e}^{-T_{\ell_i}\sigma_\mu}\cos(T_{\ell_i}\omega_\mu)$$

$$+2f_c\sum_{j=1}^{m}(-1)^{j+1}\mathrm{e}^{-T_{k_j}\sigma_\mu}\cos(T_{k_j}\omega_\mu) \tag{11}$$

$$0 = (U + f_c)\mathrm{e}^{-t_f\sigma_\mu}\sin(t_f\omega_\mu) + 2U\sum_{i=1}^{n}(-1)^i\,\mathrm{e}^{-T_{\ell_i}\sigma_\mu}\sin(T_{\ell_i}\omega_\mu)$$

$$+2f_c\sum_{j=1}^{m}(-1)^{j+1}\mathrm{e}^{-T_{k_j}\sigma_\mu}\sin(T_{k_j}\omega_\mu) \tag{12}$$

for $\mu = 1\ldots(p-1)$, where p is the number of masses. The next constraint comes from ensuring that the final boundary condition on position is satisfied. This can be found by using the final value theorem. The final value theorem can be represented as

$$x_s(t_f) = \lim_{s\to 0} G(s)G_p(s) \tag{13}$$

where $G_p(s)$ is the transfer function of the sth mass position output to the net input derived from Equation (8). For rest-to-rest maneuvers, final position of the each mass must be the same. *L'Hôpital's* rule is used to solve Equation (13). The next m constraints are the velocity constraints at the time when the friction sign changes, which are shown in the following equation:

$$v_j(t) = \mathscr{L}^{-1}[G(s)G_p(s)]|_{T_{k_j}} = 0, \quad j = 1\ldots m \tag{14}$$

There are a total of $2p+m$ constraints with $n+m+1$ unknowns (i.e. the switch and final times). `Matlab`'s optimization toolbox is used to solve for the unknown switch and final times while minimizing the final time subject to Equations (10)–(14).

4. COMPARISON WITH THE INPUT SHAPING TECHNIQUE

Because the input shaping and time-delay filter techniques are essentially identical, input shaping approach can also be used to implement the idea of friction compensation. The input shaping technique is illustrated in Figure 3 for the time-optimal control design of a benchmark two-mass–spring system. Without friction, which is shown in Figure (3)(a), the resulting control from the impulses with amplitudes of $A = [U \;\; -2U \;\; 2U \;\; -2U \;\; U]$ is a bang-bang control. The unknown switch and final times, $T = [T_1 \;\; T_2 \;\; T_3 \;\; T_f]$, are determined to eliminate the residual vibration at the final time and satisfy the boundary conditions of the maneuver.

Figure 3(b) illustrates the input shaping method in the presence of friction on the first mass. Instead of shaping the actual input, the control is shaped including the friction forces, which will result in a net control input. The velocity information of the frictional body is approximated from the solution without friction, which will be used to determine the sequence of the impulses. When there is a change in the direction of the maneuver of the frictional body,

DOI: 10.1002/oca

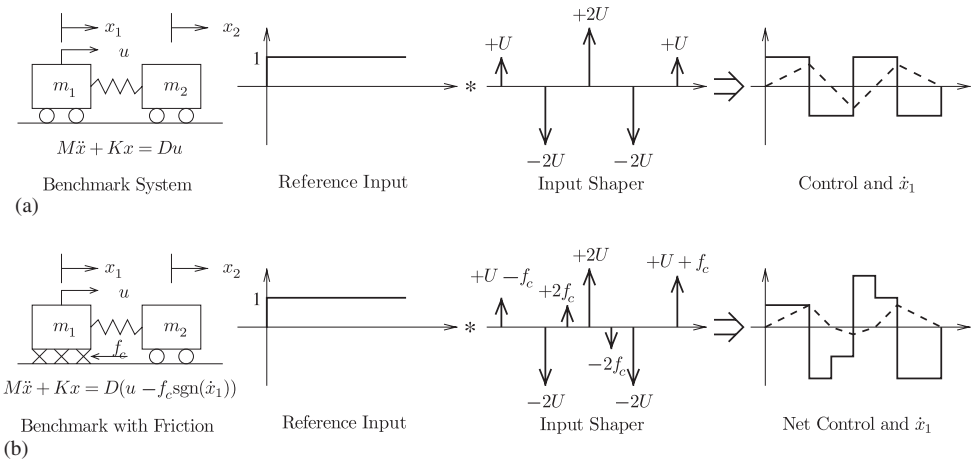

Figure 3. Input shaping and friction-compensated input shaping for time-optimal control design of benchmark two-mass–spring system: (a) time-optimal control of a benchmark two-mass–spring system using input shaping and (b) time-optimal control of two-mass–spring system under friction using input shaping.

there will be additional impulses caused by the friction value changes. Given the impulse sequences $A = [(U - f_c), -2U, 2f_c, 2U, -2f_c, -2U, (U + f_c)]$, the switch and final times, $T = [T_1\ T_2\ T_3\ T_4\ T_5\ T_f]$, are determined to eliminate vibration and satisfy the boundary conditions of the maneuver. For the friction-compensated input shapers, additional constraints are required such that the velocity of the frictional body should be zero when the frictional impulse occurs.

5. OPTIMALITY CONDITION

The time-optimal control problem with the time-delay filter approach in Section 3 is given as

$$\begin{aligned} \min \quad & \int_0^{t_f} \mathrm{d}t \\ \text{s.t.} \quad & \underline{\dot{x}} = A\underline{x} + B(u + (-1)^j f_c), \quad T_{k_{j-1}} < t < T_{k_j} \\ & \dot{x}_s(T_{k_j}) = 0 \\ & \underline{x}(0) = \underline{x}_0 \quad \text{and} \quad \underline{x}(t_f) = \underline{x}_f \\ & -U \leqslant u \leqslant U \end{aligned} \tag{15}$$

for $j = 1 \ldots m$ and $T_0 = 0$. It is assumed in Equation (15) that the frictional mass starts to maneuver from rest in the positive direction with positive velocity. Equation (15) has additional interior point constraints when the velocity of the frictional body is zero compared with the initial problem

DOI: 10.1002/oca

statement in Equation (1). The Lagrangian of this problem can be written as [18]

$$L = \underline{v}^{\mathrm{T}} \underline{N} + \int_0^{t_f} (H - \underline{\lambda}^{\mathrm{T}} \underline{\dot{x}})\, \mathrm{d}t \tag{16}$$

where

$$\begin{aligned} \text{Hamiltonian} \quad & \mathbf{H} = 1 + \underline{\lambda}^{\mathrm{T}}(A\underline{x} + B(u + (-1)^j f_{\mathrm{c}})), \quad T_{k_{j-1}} < t < T_{k_j} \\ \text{Interior point constraint} \quad & \underline{N} = [\dot{x}_s(T_{k_1}) \;\; \dot{x}_s(T_{k_2}) \;\; \ldots \;\; \dot{x}_s(T_{k_m})]^{\mathrm{T}} = \underline{0} \end{aligned} \tag{17}$$

for $j = 1 \ldots m$, and the Lagrangian multipliers are defined as

$$v_j \begin{cases} \geqslant 0 & t = T_{k_j}, \quad j = 1 \ldots m \\ = 0 & \text{elsewhere} \end{cases} \tag{18}$$

Since the Hamiltonian is not explicitly a function of time, it is equal to zero for all time t [19]. As in the system shown in Equation (1), the switching function for a new problem is also given as $B^{\mathrm{T}}\underline{\lambda}(t)$. It is also known that for optimality, the switching function must cross zero at the switching times such that

$$B^{\mathrm{T}}\underline{\lambda}(T_{\ell_i}) = 0, \quad i = 1 \ldots n \tag{19}$$

The co-state equation from the optimality condition becomes

$$\dot{\underline{\lambda}} = -\frac{\partial \mathbf{H}}{\partial \underline{x}} = -A^{\mathrm{T}}\underline{\lambda} \quad \text{for all time except } t = T_{k_j}, \quad j = 1 \ldots m \tag{20}$$

when $t = T_{k_j}$, the co-states should satisfy the following equations:

$$\begin{aligned} \underline{\lambda}(T_{k_j}^-) &= \underline{\lambda}(T_{k_j}^+) + v_j \frac{\partial N_j}{\partial \underline{x}(T_{k_j})}, \quad j = 1 \ldots m \\ \mathbf{H}(T_{k_j}^-) &= \mathbf{H}(T_{k_j}^+) - v_j \frac{\partial N_j}{\partial T_{k_j}} \end{aligned} \tag{21}$$

Since $\underline{N}$ is not explicitly a function of time, the Hamiltonian should be continuous such that $\mathbf{H}(T_{k_j}^-) = \mathbf{H}(T_{k_j}^+)$. Therefore, jump discontinuity in the co-state has to be chosen to satisfy the continuous Hamiltonian requirements, which can be written in the form

$$v_j \frac{\partial N_j}{\partial \underline{x}(T_{k_j})} = \gamma_j B^{\mathrm{T}} \underline{\lambda}(T_{k_j}^-) \tag{22}$$

Once the v_j's are determined, an expression for $\underline{\lambda}(T_{\ell_i})$ in terms of the initial co-states, $\underline{\lambda}(0)$, can be determined from Equations (20) and (21). Then the switching function at the control switches is established in terms of $\underline{\lambda}(0)$ as shown in Equation (19). As an example, assume that the first time that the velocity goes to zero is T_{k_1}, then the co-states at $T_{k_1}^-$ are given by the following equation:

$$\underline{\lambda}(T_{k_1}^-) = \mathrm{e}^{-A^{\mathrm{T}} T_{k_1}^-} \underline{\lambda}(0) \tag{23}$$

DOI: 10.1002/oca

The co-states at $t = T_{k_1}^+$ are given as

$$\underline{\lambda}(T_{k_1}^+) = (\mathscr{I} + J_1)\underline{\lambda}(T_{k_1}^-) = (\mathscr{I} + J_1)\underline{\lambda}(T_{k_1}^-)\mathrm{e}^{-A^{\mathrm{T}}T_{k_1}^-}\underline{\lambda}(0) \tag{24}$$

where J_1 is a $2p \times 2p$ matrix where $(p+s)$th row is $-\gamma_1 B^{\mathrm{T}}$ and zeros for the rest, and $\mathscr{I}$ is a $2p \times 2p$ identity matrix. Then the co-states can be integrated until the next switch with these new initial conditions. This procedure is repeated until the $n \times 2p$ matrix $\mathscr{M}$ is formed for n switch times such that

$$\begin{bmatrix} B^{\mathrm{T}}\underline{\lambda}(T_{\ell_1}) \\ B^{\mathrm{T}}\underline{\lambda}(T_{\ell_2}) \\ \vdots \\ B^{\mathrm{T}}\underline{\lambda}(T_{\ell_n}) \end{bmatrix} = \mathscr{M}\underline{\lambda}(0) = \underline{0} \tag{25}$$

$\underline{\lambda}(0)$ is found by the null space of $\mathscr{M}$ which satisfies the Hamiltonian requirements such that $\mathbf{H}(t=0) = 0$. After calculating $\underline{\lambda}(0)$ from Equation (25), the co-states can then be integrated forward and the resulting switching function must cross zero at the switching time to ensure optimality.

6. NUMERICAL EXAMPLE

The example problem considered is illustrated in Figure 4. The control input and Coulomb friction forces are acting on the first mass. The time-optimal control problem can be stated as

$$\begin{aligned} &\min \quad \int_0^{t_f} \mathrm{d}t \\ &\text{s.t.} \\ &\dot{\underline{x}}(t) = \begin{bmatrix} 0 & 0 & 1 & 0 \\ 0 & 0 & 0 & 1 \\ -1 & 1 & 0 & 0 \\ 0.5 & -0.5 & 0 & 0 \end{bmatrix} \underline{x}(t) + \begin{bmatrix} 0 \\ 0 \\ 1 \\ 0 \end{bmatrix} (u - f_{\mathrm{c}}\,\mathrm{sign}(x_3)) \\ &\underline{x}(0) = [0\ \ 0\ \ 0\ \ 0]^{\mathrm{T}}, \quad \underline{x}(t_f) = [1\ \ 1\ \ 0\ \ 0]^{\mathrm{T}} \quad \text{and} \quad -1 \leqslant u \leqslant 1 \end{aligned} \tag{26}$$

With the knowledge that the time-optimal control profile of the linear undamped two-mass–spring system has three switches and two zero velocity crossings [6], we assume $n = 3$, $m = 2$, $k = [2\ \ 4]$, and $\ell = [1\ \ 3\ \ 5]$. The flexible poles are given by $s = \pm\omega i$, where $\omega = \sqrt{1.5}$. The net control input is parameterized as shown in Figure 2. Then the parameter optimization problem can be stated as

$$\min t_f \tag{27}$$

subject to the switch time constraints,

$$0 \leqslant T_1 \leqslant T_2 \leqslant T_3 \leqslant T_4 \leqslant T_5 \leqslant t_f \tag{28}$$

DOI: 10.1002/oca

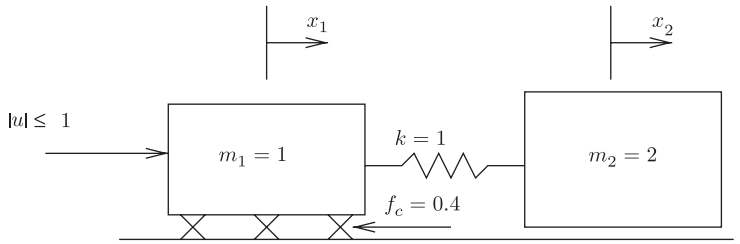

Figure 4. Two-mass–spring system subject to Coulomb friction.

rigid body pole cancellation constraint,

$$2T_1 - 2f_cT_2 - 2T_3 + 2f_cT_4 + 2T_5 - (1 + f_c)t_f = 0 \tag{29}$$

flexible body pole cancellation constraints,

$$\begin{aligned}(1 - f_c) - 2\cos(\omega T_1) + 2f_c\cos(\omega T_2) + 2\cos(\omega T_3)\\ - 2f_c\cos(\omega T_4) - 2\cos(\omega T_5) + (1 + f_c)\cos(\omega t_f) = 0\end{aligned} \tag{30}$$

$$\begin{aligned}-2\sin(\omega T_1) + 2f_c\sin(\omega T_2) + 2\sin(\omega T_3)\\ - 2f_c\sin(\omega T_4) - 2\sin(\omega T_5) + (1 + f_c)\sin(\omega t_f) = 0\end{aligned} \tag{31}$$

final displacement constraint,

$$\tfrac{1}{4}(-2T_1^2 + 2f_cT_2^2 + 2T_3^2 - 2f_cT_4^2 - 2T_5^2 + (1 + f_c)t_f^2) = 1 \tag{32}$$

and first mass velocity constraints,

$$\frac{1}{m_1 + m_2}\left[(1 - f_c)\left(\frac{m_2}{m_1\omega}\sin(\omega T_2) + T_2\right) - 2\left(\frac{m_2}{m_1\omega}\sin(\omega(T_{21})) + (T_{21})\right)\right] = 0 \tag{33}$$

$$\begin{aligned}\frac{1}{m_1 + m_2}\Bigg[(1 - f_c)\left(\frac{m_2}{m_1\omega}\sin(\omega T_4) + T_4\right) - 2\left(\frac{m_2}{m_1\omega}\sin(\omega(T_{41})) + (T_{41})\right)\\ + 2f_c\left(\frac{m_2}{m_1\omega}\sin(\omega(T_{42})) + (T_{42})\right) + 2\left(\frac{m_2}{m_1\omega}\sin(\omega(T_{43})) + (T_{43})\right)\Bigg] = 0\end{aligned} \tag{34}$$

where T_{ab} stands for $T_a - T_b$ in Equations (33) and (34). The constrained nonlinear optimizer of `MatLab` was used to solve this problem. The time-delay filter is found to be

$$G(s) = 0.6 - 2e^{-1.8164s} + 0.8e^{-2.1177s} + 2e^{-3.1498s} - 0.8e^{-3.5918s} - 2e^{-4.4047s} + 1.4e^{-5.2298s} \tag{35}$$

With the resulting control input, the time-optimal control profile and the two mass positions are plotted on the bottom figures of Figure 5. The top figure shows the time-optimal control profile and two mass positions without the consideration of the frictional effect. It is shown that without

DOI: 10.1002/oca

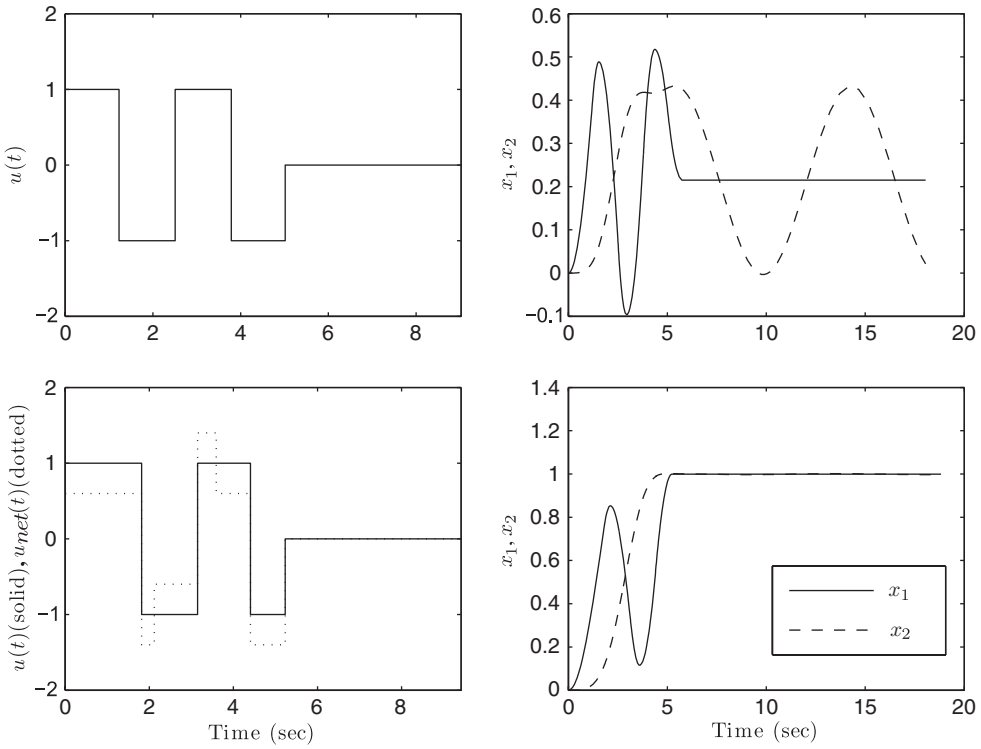

Figure 5. Comparison of control profile and states with and without friction compensation.

the friction compensation in the control input, the first mass will show displacement error and the second mass will show undesirable vibrations at the end of the maneuver. Co-states and switching curve can be computed with the resulting control profile to determine the optimality. The Hamiltonian of the problem is

$$\mathbf{H} = \begin{cases} 1 + \underline{\lambda}^{\mathrm{T}}(A\underline{x} + B(u - f_{\mathrm{c}})), & 0 < t < T_2 \\ 1 + \underline{\lambda}^{\mathrm{T}}(A\underline{x} + B(u + f_{\mathrm{c}})), & T_2 < t < T_4 \\ 1 + \underline{\lambda}^{\mathrm{T}}(A\underline{x} + B(u - f_{\mathrm{c}})), & T_4 < t < t_f \end{cases} \tag{36}$$

and the interior point constraints are

$$N_1 = \dot{x}_1(T_2) = 0 \quad \text{and} \quad N_2 = \dot{x}_1(T_4) = 0 \tag{37}$$

The Hamiltonian should be continuous such that $\mathbf{H}(T_2^+) = \mathbf{H}(T_2^-)$ and $\mathbf{H}(T_4^+) = \mathbf{H}(T_4^-)$. The switching function is $B^{\mathrm{T}}\underline{\lambda} = \lambda_3$ and there is a discontinuity only in λ_3. The continuous Hamiltonian

DOI: 10.1002/oca

requirement yields

$$1 + [\lambda_1(T_2)\,\lambda_2(T_2)\,\lambda_3(T_2^-)\,\lambda_4(T_2)](A\underline{x}(T_2) + B(-1 - f_c))$$
$$= 1 + [\lambda_1(T_2)\,\lambda_2(T_2)\,\lambda_3(T_2^+)\,\lambda_4(T_2)](A\underline{x}(T_2) + B(-1 + f_c)) \quad (38)$$

$$1 + [\lambda_1(T_4)\,\lambda_2(T_4)\,\lambda_3(T_4^-)\,\lambda_4(T_4)](A\underline{x}(T_4) + B(1 + f_c))$$
$$= 1 + [\lambda_1(T_4)\,\lambda_2(T_4)\,\lambda_3(T_4^+)\,\lambda_4(T_4)](A\underline{x}(T_4) + B(1 - f_c)) \quad (39)$$

Assuming $\lambda_3(T_2^+)=\lambda_3(T_2^-)+\gamma_1\lambda_3(T_2^-)$ and $\lambda_3(T_4^+)=\lambda_3(T_4^-)+\gamma_2\lambda_3(T_4^-)$, γ_1 and γ_2 are found to be

$$\gamma_1 = \frac{-2f_c}{-1 + f_c - k(x_1(T_2) - x_2(T_2))} \quad \text{and} \quad \gamma_2 = \frac{2f_c}{1 - f_c - k(x_1(T_4) - x_2(T_4))} \quad (40)$$

From the equation, the co-states at the switch times are found in terms of $\underline{\lambda}(0)$ such that

$$\begin{aligned}
\underline{\lambda}(T_1) &= \mathrm{e}^{-A^{\mathrm{T}}T_1}\underline{\lambda}(0)\\
\underline{\lambda}(T_2^-) &= \mathrm{e}^{-A^{\mathrm{T}}(T_2-T_1)}\underline{\lambda}(T_1)\\
\underline{\lambda}(T_2^+) &= (I + J_1)\underline{\lambda}(T_2^-)\\
\underline{\lambda}(T_3) &= \mathrm{e}^{-A^{\mathrm{T}}(T_3-T_2)}\underline{\lambda}(T_2^+)\\
\underline{\lambda}(T_4^-) &= \mathrm{e}^{-A^{\mathrm{T}}(T_4-T_3)}\underline{\lambda}(T_3)\\
\underline{\lambda}(T_4^+) &= (I + J_2)\underline{\lambda}(T_4^-)\\
\underline{\lambda}(T_5) &= \mathrm{e}^{-A^{\mathrm{T}}(T_5-T_4)}\underline{\lambda}(T_4^+)
\end{aligned} \quad (41)$$

where J_1 and J_2 are defined as

$$J_1 = \begin{bmatrix} 0 & 0 & 0 & 0 \\ 0 & 0 & 0 & 0 \\ 0 & 0 & \gamma_1 & 0 \\ 0 & 0 & 0 & 0 \end{bmatrix} \quad \text{and} \quad J_2 = \begin{bmatrix} 0 & 0 & 0 & 0 \\ 0 & 0 & 0 & 0 \\ 0 & 0 & \gamma_2 & 0 \\ 0 & 0 & 0 & 0 \end{bmatrix} \quad (42)$$

$\mathscr{M}$ is now given to satisfy $\mathscr{M}\underline{\lambda}(0) = \underline{0}$ such that

$$\mathscr{M} = \begin{bmatrix} B^{\mathrm{T}}\mathrm{e}^{-A^{\mathrm{T}}T_1} \\ B^{\mathrm{T}}\mathrm{e}^{-A^{\mathrm{T}}(T_3-T_2)}(I + J_1)\mathrm{e}^{-A^{\mathrm{T}}(T_2-T_1)}\mathrm{e}^{-A^{\mathrm{T}}T_1} \\ B^{\mathrm{T}}\mathrm{e}^{-A^{\mathrm{T}}(T_5-T_4)}(I + J_2)\mathrm{e}^{-A^{\mathrm{T}}(T_4-T_3)}\mathrm{e}^{-A^{\mathrm{T}}(T_3-T_2)}(I + J_1)\mathrm{e}^{-A^{\mathrm{T}}(T_2-T_1)}\mathrm{e}^{-A^{\mathrm{T}}T_1} \end{bmatrix} \quad (43)$$

DOI: 10.1002/oca

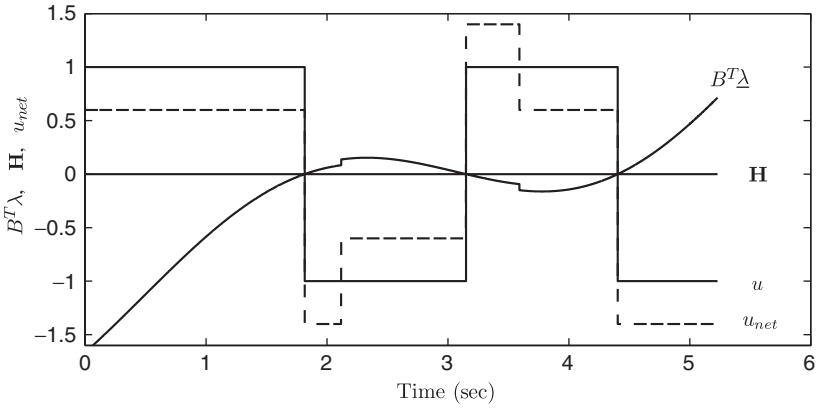

Figure 6. Linearizing control input, switching function, and Hamiltonian.

The initial co-states are found to satisfy $\mathscr{M}\underline{\lambda}(0) = \underline{0}$ and $\mathbf{H}(t = 0) = 0$ such that

$$\underline{\lambda}(0) = -\frac{\text{Null}(\mathscr{M})}{[\text{Null}(\mathscr{M})]^{\text{T}} B(1 - f_{\text{c}})} \tag{44}$$

where Null($\mathscr{M}$) is the null space of $\mathscr{M}$. The linearizing input as well as the switching curve is shown in Figure 6 for the example problem. The actual input is found by subtracting the friction force from the net input.

7. VARIATION OF CONTROL STRUCTURE AS A FUNCTION OF FINAL POSITION

In the previous example, the velocity of the first mass is zero at T_2 and T_4. As the final position increases for the previous example, the time gap between T_3 and T_4 becomes small until they coincide. The control profile for this transition shown in Figure 7 indicates that the velocity crossing coincides with the control switch which will result in a four-switch control profile. The transition displacement for this example is $d \approx 3.4$. After the transition displacement, going back to original profile does not provide a feasible solution. Also, keeping the four-switch transition profile shown in Figure 7 with the increased terminal displacement creates an over-constrained problem and does not provide feasible solutions. Therefore, the velocity of the first mass should cross zero before the new control switch activates. This implies that now T_3 is the time when the velocity is zero and T_4 is the time when the control switches. At T_3^+, the velocity becomes positive and therefore friction force becomes $-f_{\text{c}}$. However, the linearizing input with the new friction value drives the first mass to the negative direction if the net input is less than zero. Once the first mass crosses the zero velocity, the net input changes its sign again because of the change in friction value to $+f_{\text{c}}$. This will continue until the forces of the frictional body overcome the friction force. Since applied forces to the first mass are not large enough to overcome friction, the velocity of the first mass stays zero until the new control switch is activated to overcome friction. In this stiction period, the friction force becomes

$$f = u + k(x_2 - x_1) \quad \text{if } \dot{x}_1 = 0 \text{ and } f \leqslant f_{\text{c}} \tag{45}$$

DOI: 10.1002/oca

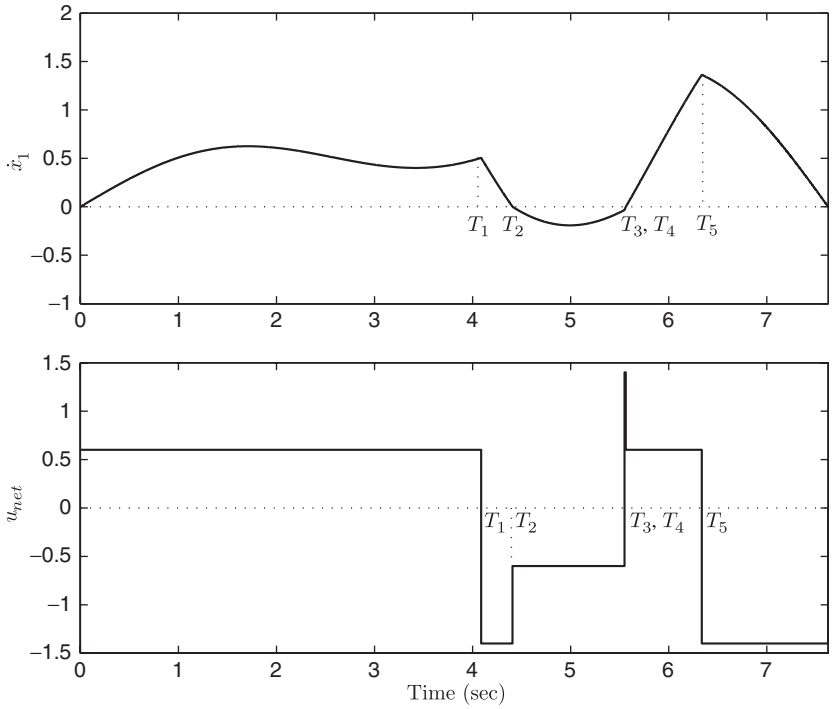

Figure 7. Velocity and control input profiles at the transition.

One way to formulate an optimal control problem with stiction is adding an additional constraint to the problem such that the velocity of the first mass is zero for this time interval. For the example problem, the predicted velocity profile of the first mass is plotted in Figure 8 showing that the velocity of the first mass is zero until the new switch actuates. It is also possible that the spring force itself can overcome the friction force before the new control switch happens, which will require an additional constraint satisfying the condition that the spring force is equal to Coulomb friction value at the exit of the zero velocity. With the velocity profile in Figure 8, the new optimal control problem can be formulated as

$$\begin{aligned}
\min \quad & \int_0^{T_f} \mathrm{d}t \\
\text{s.t.} \quad & \dot{\underline{x}} = A\underline{x} + B(u - f_c), \quad 0 < t < T_2 \\
& \dot{\underline{x}} = A\underline{x} + B(u + f_c), \quad T_2 < t < T_3 \\
& \dot{\underline{x}} = A\underline{x} + Bu, \quad T_3 < t < T_4 \\
& \dot{\underline{x}} = A\underline{x} + B(u - f_c), \quad T_4 < t < T_f \\
& \dot{x}_1 = 0, \quad t = T_2 \text{ and } T_3 < t < T_4 \\
& \underline{x}(0) = \underline{x}_0 \quad \text{and} \quad \underline{x}(T_f) = \underline{x}_f \\
& -1 \leqslant u \leqslant 1
\end{aligned} \tag{46}$$

DOI: 10.1002/oca

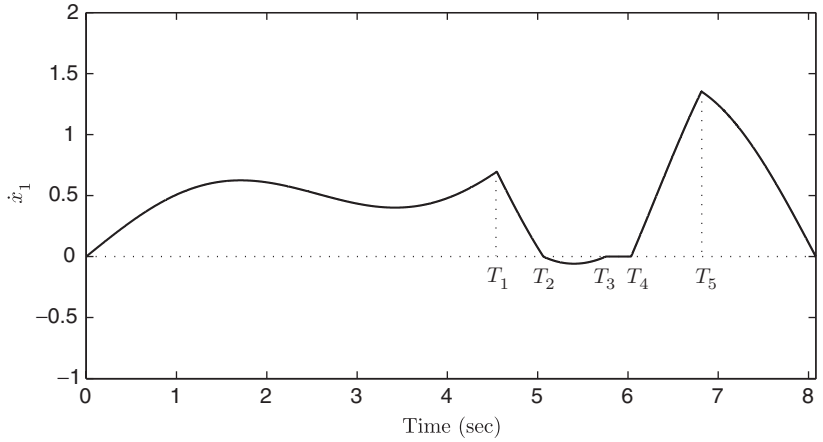

Figure 8. Velocity and control input profiles after transition displacement.

Equation (46) has a state equality constraint on the velocity of the first mass. Because of this constraint, the friction force during stiction is considered zero. Bryson and Ho [18] have developed a method to handle the state equality constraints in the optimal control problem. From [18], Equation (46) can be reformulated as

$$
\begin{aligned}
\min \quad & \int_0^{T_f} \mathrm{d}t \\
\text{s.t.} \quad & \dot{\underline{x}} = A\underline{x} + B(u - f_c), \quad 0<t<T_2 \\
& \dot{\underline{x}} = A\underline{x} + B(u + f_c), \quad T_2<t<T_3 \\
& \dot{\underline{x}} = A\underline{x} + Bu, \quad T_3<t<T_4 \\
& \dot{\underline{x}} = A\underline{x} + B(u - f_c), \quad T_4<t<T_f \\
& \ddot{x}_1 = \frac{k}{m_1}(x_2 - x_1) + u = 0, \quad T_3<t<T_4 \\
& \dot{x}_1(T_2) = \dot{x}_1(T_3) = 0 \\
& \underline{x}(0) = \underline{x}_0 \quad \text{and} \quad \underline{x}(T_f) = \underline{x}_f \\
& -1 \leqslant u \leqslant 1
\end{aligned}
\tag{47}
$$

Because the friction force is zero for the zero velocity, the control for $T_3<t<T_4$ should satisfy the equality constraint in Equation (47) such that

$$u = \frac{k}{m_1}(x_1 - x_2), \quad T_3<t<T_4 \tag{48}$$

It is interesting to see that although the control input needed to stay stuck for $T_3<t<T_4$ is defined by Equation (48), because of the assumption of stiction during the interval, it is possible to use constant control input value of $u=-1$. Now, the control profile can be parameterized from the predicted velocity profile including the state constraint effect of stiction. The time-delay filter

DOI: 10.1002/oca

cannot be used for this profile because of the feedback control effect in the chattering interval. When Equation (48) is substituted into Equation (47), the system's A matrix is altered for time $T_3 < t < T_4$. However, the control profile can be used to integrate the system forward in time using the given initial guesses of the switch times to obtain the states at the switch and final times

$$\begin{aligned}
\underline{x}(T_1) &= \mathrm{e}^{AT_1}\underline{x}_0 + \int_0^{T_1} \mathrm{e}^{A(t-\tau)}B(1-f_\mathrm{c})\,\mathrm{d}\tau \\
\underline{x}(T_2) &= \mathrm{e}^{A(T_2-T_1)}\underline{x}(T_1) + \int_{T_1}^{T_2} \mathrm{e}^{A(t-\tau)}B(-1-f_\mathrm{c})\,\mathrm{d}\tau \\
\underline{x}(T_3) &= \mathrm{e}^{A(T_3-T_2)}\underline{x}(T_2) + \in \int_{T_2}^{T_3} \mathrm{e}^{A(t-\tau)}B(-1+f_\mathrm{c})\,\mathrm{d}\tau \\
\underline{x}(T_4) &= \mathrm{e}^{A^\mathrm{c}(T_4-T_3)}\underline{x}(T_3) \\
\underline{x}(T_5) &= \mathrm{e}^{A(T_5-T_4)}\underline{x}(T_4) + \int_{T_4}^{T_5} \mathrm{e}^{A(t-\tau)}B(1-f_\mathrm{c})(\tau)\,\mathrm{d}\tau \\
\underline{x}(T_f) &= \mathrm{e}^{A(T_6-T_5)}\underline{x}(T_5) + \int_{T_5}^{T_6} \mathrm{e}^{A(t-\tau)}B(-1-f_\mathrm{c})(\tau)\,\mathrm{d}\tau
\end{aligned} \tag{49}$$

where A^c is the closed loop system equation in the interval at $t \in [T_3,\ T_4]$ using Equation (48)

$$A^\mathrm{c} = \begin{bmatrix} 0 & 0 & 1 & 0 \\ 0 & 0 & 0 & 1 \\ 0 & 0 & 0 & 0 \\ \dfrac{k}{m_2} & -\dfrac{k}{m_2} & 0 & 0 \end{bmatrix} \tag{50}$$

For computational accuracy and convenience, it is very useful to use the following property to compute the states at the switch times:

$$\exp\left(\begin{bmatrix} A & B \\ 0 & 0 \end{bmatrix} t\right) = \begin{bmatrix} \mathrm{e}^{At} & \displaystyle\int_0^t \mathrm{e}^{A(t-\tau)}B\,\mathrm{d}\tau \\ 0 & 1 \end{bmatrix} \tag{51}$$

Now the problem can be solved for switch times numerically by minimizing the final time T_6 with the constraints

$$\begin{aligned}
&\dot{x}_1(T_2) = 0 \\
&\dot{x}_1(T_3) = 0 \\
&\underline{x}(T_f) = [x_1(T_f) \quad x_2(T_f) \quad 0 \quad 0]^\mathrm{T}
\end{aligned} \tag{52}$$

The resulting control profile is used to verify the optimality of the control input by inspecting the optimality conditions. The Lagrangian for this problem can be formulated as [18]

$$L = \psi N_1 + \pi N_2 + \int_{t_0}^{T_f} (\mathbf{H} - \underline{\lambda}^\mathrm{T}\underline{\dot{x}})\,\mathrm{d}t \tag{53}$$

DOI: 10.1002/oca

where

$$\begin{aligned}
\text{Hamiltonian} \quad & \mathbf{H} = 1 + \underline{\lambda}^{\mathrm{T}}(A\underline{x} + B(u - f_{\mathrm{c}})), \quad 0 < t < T_2 \\
& \mathbf{H} = 1 + \underline{\lambda}^{\mathrm{T}}(A\underline{x} + B(u + f_{\mathrm{c}})), \quad T_2 < t < T_3 \\
& \mathbf{H} = 1 + \underline{\lambda}^{\mathrm{T}}(A\underline{x} + Bu) + \mu C, \quad T_3 < t < T_4 \\
& \mathbf{H} = 1 + \underline{\lambda}^{\mathrm{T}}(A\underline{x} + B(u - f_{\mathrm{c}})), \quad T_4 < t < T_f \\
\text{Interior point constraint} \quad & N_1 = \dot{x}_1(T_2) = 0 \\
& N_2 = \dot{x}_1(T_3) = 0 \\
\text{Equality constraint} \quad & C = \ddot{x}_1(t) = k(x_2 - x_1) + u = 0
\end{aligned} \tag{54}$$

and the Lagrangian multipliers are defined as

$$\mu \begin{cases} \geqslant 0, & t \in [T_3,\ T_4] \\ = 0 & \text{elsewhere} \end{cases}, \quad \psi \begin{cases} \geqslant 0, & t = T_2 \\ = 0 & \text{elsewhere} \end{cases} \quad \text{and} \quad \pi \begin{cases} \geqslant 0, & t = T_3 \\ = 0 & \text{elsewhere} \end{cases} \tag{55}$$

The input u is considered to be within the saturation limit for $T_3 < t < T_4$ because of the stiction assumption with $u = -1$. Then, μ can be found from the following relationship:

$$\frac{\partial \mathbf{H}}{\partial u} = 0 = B^{\mathrm{T}}\underline{\lambda} + \mu \quad \text{or} \quad \mu = -B^{\mathrm{T}}\underline{\lambda}, \quad T_3 < t < T_4 \tag{56}$$

Therefore, the co-state equation is found from Equation (56) and the necessary optimality condition

$$\dot{\underline{\lambda}} = -\frac{\partial \mathbf{H}}{\partial \underline{x}} = \begin{cases} \left(-A^{\mathrm{T}} + \dfrac{\partial C}{\partial \underline{x}} B^{\mathrm{T}}\right)\underline{\lambda}, & T_3 < t < T_4 \\ -A^{\mathrm{T}}\underline{\lambda} & \text{elsewhere except } t = T_2 \quad \text{and} \quad t = T_3 \end{cases} \tag{57}$$

At the interior points, $t = T_2$ and T_3, the co-states become discontinuous by the following equations:

$$\begin{aligned}
\underline{\lambda}(T_2^-) &= \underline{\lambda}(T_2^+) + \psi \frac{\partial N_1}{\partial \underline{x}(T_2)} \\
\mathbf{H}(T_2^-) &= \mathbf{H}(T_2^+) - \psi \frac{\partial N_1}{\partial T_2}
\end{aligned} \quad \text{and} \quad \begin{aligned}
\underline{\lambda}(T_3^-) &= \underline{\lambda}(T_3^+) + \pi \frac{\partial N_2}{\partial \underline{x}(T_3)} \\
\mathbf{H}(T_3^-) &= \mathbf{H}(T_3^+) - \pi \frac{\partial N_2}{\partial T_3}
\end{aligned} \tag{58}$$

Since the interior point constraints are not explicit functions of time, the Hamiltonian is continuous such that $\mathbf{H}(T_2^-) = \mathbf{H}(T_2^+)$ and $\mathbf{H}(T_3^-) = \mathbf{H}(T_3^+)$. Therefore, ψ and π in Equation (58) are chosen to satisfy the continuous Hamiltonian requirement that will yield the following equations:

$$\gamma_1 = \frac{-2 f_{\mathrm{c}}}{-1 + f_{\mathrm{c}} - k(x_1(T_2) - x_2(T_2))} \quad \text{and} \quad \lambda_3(T_3^-) = 0 \tag{59}$$

DOI: 10.1002/oca

where γ_1 satisfies $\lambda_3(T_2^+) = \lambda_3(T_2^-) + \gamma_1 \lambda_3(T_2^-)$. Co-states can be integrated forward in time with the initial $\underline{\lambda}(0)$ using Equation (57) and (59).

$$\begin{aligned}
\underline{\lambda}(T_1) &= \mathrm{e}^{-A^{\mathrm{T}}T_1}\underline{\lambda}(0) \\
\underline{\lambda}(T_2^-) &= \mathrm{e}^{-A^{\mathrm{T}}(T_2-T_1)}\underline{\lambda}(T_1) \\
\underline{\lambda}(T_2^+) &= (I + J_1)\underline{\lambda}(T_2^-) \\
\underline{\lambda}(T_3^-) &= \mathrm{e}^{-A^{\mathrm{T}}(T_3-T_2)}\underline{\lambda}(T_2^+) \\
\underline{\lambda}(T_3^+) &= (I + J_2)\underline{\lambda}(T_3^-) \\
\underline{\lambda}(T_4) &= \mathrm{e}^{(-A^{\mathrm{T}}+\partial C/\partial \underline{x})(T_4-T_3)}\underline{\lambda}(T_3^+) \\
\underline{\lambda}(T_5) &= \mathrm{e}^{-A^{\mathrm{T}}(T_5-T_4)}\underline{\lambda}(T_4)
\end{aligned} \tag{60}$$

where I is an 4×4 identity matrix and

$$J_1 = \begin{bmatrix} 0 & 0 & 0 & 0 \\ 0 & 0 & 0 & 0 \\ 0 & 0 & \gamma_1 & 0 \\ 0 & 0 & 0 & 0 \end{bmatrix} \quad \text{and} \quad J_2 = \begin{bmatrix} 0 & 0 & 0 & 0 \\ 0 & 0 & 0 & 0 \\ 0 & 0 & \infty & 0 \\ 0 & 0 & 0 & 0 \end{bmatrix} \tag{61}$$

Because $\underline{\lambda}(T_3^-)$ should be zero, an infinite value has to multiply $\underline{\lambda}(T_3^-)$ in J_2 to have finite jump discontinuities in the co-states. For numerical computations, a large number is used in J_2 instead of ∞. Since the switching curve should cross zero at the actual switch times, T_1, T_4, and T_5, the following should be satisfied:

$$\mathscr{M}\underline{\lambda}(0) = \underline{0} \tag{62}$$

where

$$\mathscr{M} = \begin{bmatrix} B^{\mathrm{T}}\mathrm{e}^{-A^{\mathrm{T}}T_1} \\ B^{\mathrm{T}}\mathrm{e}^{(-A^{\mathrm{T}}+\partial C/\partial \underline{x})(T_4-T_3)}(I+J_2)\mathrm{e}^{-A^{\mathrm{T}}(T_3-T_2)}(I+J_1)\mathrm{e}^{-A^{\mathrm{T}}(T_2-T_1)}\mathrm{e}^{-A^{\mathrm{T}}T_1} \\ B^{\mathrm{T}}\mathrm{e}^{-A^{\mathrm{T}}(T_5-T_4)}\mathrm{e}^{(-A^{\mathrm{T}}+\partial C/\partial \underline{x})(T_4-T_3)}(I+J_2)\mathrm{e}^{-A^{\mathrm{T}}(T_3-T_2)}(I+J_1)\mathrm{e}^{-A^{\mathrm{T}}(T_2-T_1)}\mathrm{e}^{-A^{\mathrm{T}}T_1} \end{bmatrix} \tag{63}$$

Therefore, $\underline{\lambda}(0)$ is selected to satisfy Equation (62) and Hamiltonian requirement, $H(t=0) = 0$, such that

$$\underline{\lambda}(0) = -\frac{\mathrm{Null}(\mathscr{M})}{[\mathrm{Null}(\mathscr{P})]^{\mathrm{T}}B(1 - f_{\mathrm{c}})} \tag{64}$$

In Figure 9, the linearizing control input along with the switching curve is plotted. The Hamiltonian is also plotted which is zero for all times. The actual control input is computed by subtracting the frictional force from the linearizing control input. Because the friction force is zero when the velocity of the first mass is zero, the linearizing input is the same as the actual input in the stiction region. However, the actual control input becomes $u = -1$ for the stiction interval, since

DOI: 10.1002/oca

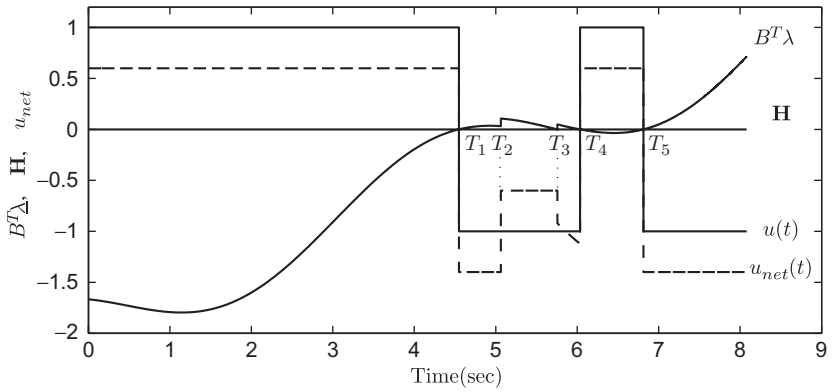

Figure 9. Linearizing control input, switching function, and Hamiltonian after transition.

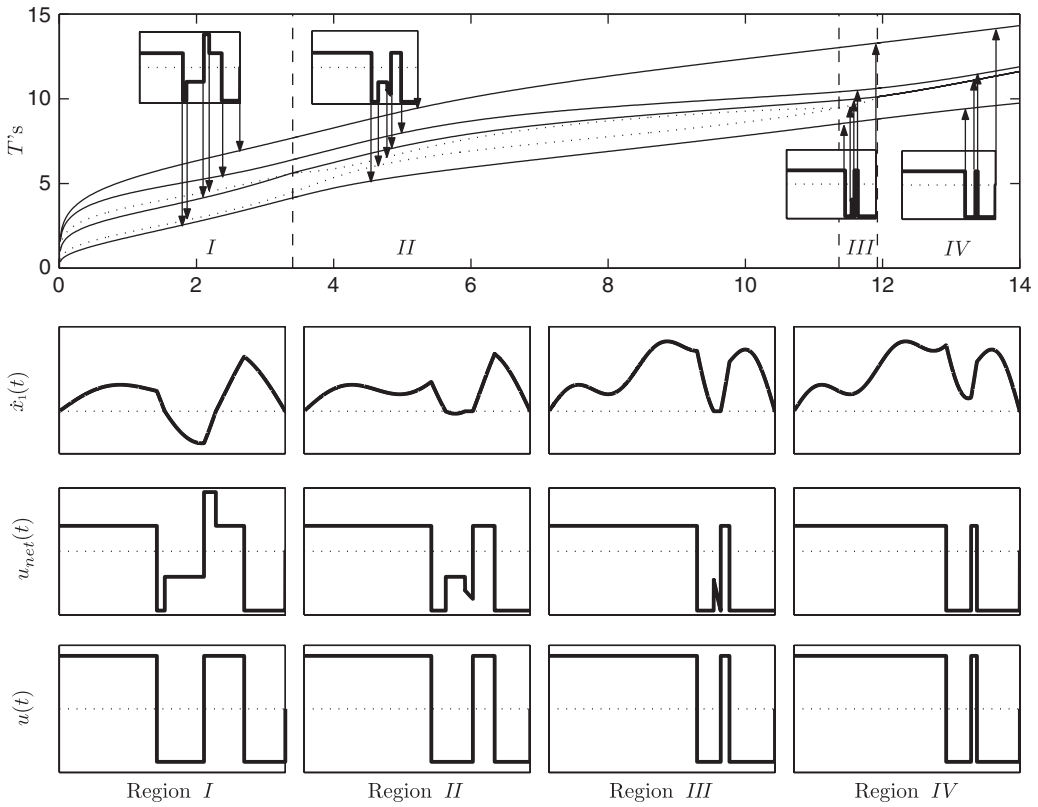

Figure 10. Switch time *vs* displacement with velocity and control input profiles.

the compensation of the spring force is not necessary to stay stuck. Therefore, the actual control input becomes a three-switch bang-bang. The resulting net control input satisfies the necessary optimality conditions as shown in Figure 9.

DOI: 10.1002/oca

As the final displacement is increased further, the profile of the control shows additional transitions. In Figure 10, the summary of the control input transition profile for the example problem is shown. The switch times are plotted as a function of final displacement showing that control switches are smooth curves for final displacement changes. The actual control switches are plotted with solid line and velocity switches are plotted with dotted line in Figure 10. The linearizing net input and actual control input profiles are also shown in Figure 10 for different displacements. In region III, the velocity of the first mass never goes negative, but stays zero for some time due to stiction. The corresponding control profile can be solved as in the previous case, when the velocity of the first mass is forced to zero during stiction. The corresponding net control input plotted in Figure 10 has four control switches without the negative velocity maneuvers of the first mass. The actual control input remains a three-switch bang-bang profile. If the final displacement is increased further, the velocity of the first mass will always stay positive during the maneuver. Consequently, the net control input can be parameterized with the three-switch bang-bang profile as shown in region IV of Figure 10, which is a Coulomb friction-biased control. The time-delay filter approach can be used for this profile since the linearizing input does not depend on the states.

8. CONCLUSION

It is shown that the linearizing net input approach provides the time-optimal control solution for the multiple-mass–spring–damper system under the assumption of correct parametrization of the control input. With the net input approach, the hard nonlinearity in the friction model is eliminated. Static friction effect can also be included in the time-optimal control design which will require that the sum of all the forces on the frictional body is greater than the static friction value when the motion is initiated from zero velocity (i.e. break out from velocity reversals). If the Stribeck or dynamic friction model is used, numerical optimization is required to integrate the system equation of motion. However, the hard nonlinearity in these models can still be overcome by parameterizing the net input. The net input parametrization technique can also extended to systems where one or more mass is under frictional forces, which will lead to multiple net input system. This will require a correct knowledge of velocity profiles of all the masses subject to the friction.

REFERENCES

1. Armstrong-Helouvry B, Dupon P, Canudas De Wit C. Survey of models, analysis tools and compensation methods for the control of machines with friction. *Automatica* 1994; **30**(7):1083–1138.
2. Scrivener SL, Thompson RC. Survey of time-optimal attitude maneuvers. *Journal of Guidance*, *Control*, *and Dynamics* 1994; **17**(2):225–233.
3. Singh G, Kambamba PT, McClanroch NH. Planar, time-optimal, rest to rest slewing maneuvers of flexible spacecraft. *Journal of Guidance*, *Control*, *and Dynamics* 1989; **12**(1):71–81.
4. Ben-Asher J, Burns JA, Cliff EM. Time-optimal slewing of flexible spacecraft. *Journal of Guidance*, *Control*, *and Dynamics* 1992; **15**(2):360–367.
5. Liu Q, Wie B. Robust time-optimal control of uncertain flexible spacecraft. *Journal of Guidance*, *Control*, *and Dynamics* 1992; **15**(3):597–604.
6. Singh T, Vadali SR. Robust time-optimal vontrol: frequency domain approach. *Journal of Guidance*, *Control*, *and Dynamics* 1994; **17**(2):346–353.
7. Singer NC, Seering WP. Preshaping command inputs to reduce system vibrations. *Journal of Dynamic Systems*, *Measurement*, *and Control* (ASME) 1990; **112**:76–82.
8. Singh T. Fuel/time optimal control of the benchmark problem. *Journal of Guidance*, *Control*, *and Dynamics* 1995; **18**(6):1225–1231.

DOI: 10.1002/oca

9. Hindle T, Singh T. Robust minimum power/jerk control of maneuvering structures. *Journal of Guidance, Control, and Dynamics* 2001; **24**(4):816–826.
10. Muenchhof M, Singh T. Desensitized jerk limited time-optimal control of multi-input systems. *Journal of Guidance, Control, and Dynamics* 2002; **25**(3):474–481.
11. Singh T, Singhose W. Tutorial on input shaping/time delay control of maneuvering flexible structures. *2002 American Control Conference*, 8–10 May, Alaska, 2002.
12. Kim T-H, Ha I-J. Time-optimal control of a single-DOF mechanical system with friction. *IEEE Transactions on Automatic Control* 2001; **46**(5):751–755.
13. Driessen BJ, Sadegh N. Minimum-time control of systems with Coulomb friction: near global optima via mixed integer linear programming. *Optimal Control Applications and Methods* 2001; **22**(2):51–62.
14. Lawrence J, Singhose W, Hekman K. Friction-compensating input shaping for vibration reduction. *Journal of Vibration and Acoustics* (ASME) 2005; **127**(4):307–314.
15. Lee HW, Jennings KL, Rehbock V. Control parametrization enhancing technique for time optimal control problems. *Dynamic Systems and Applications* 1997; **6**:243–263.
16. Kaya CY, Noakes JL. Computations and time-optimal controls. *Optimal Control Applications and Methods* 1996; **17**:171–185.
17. Khmelnitsky EA. Combinational, graph-based solution method for a class of continuous time optimal control problems. *Mathematics of Operations Research* 2002; **27**(2):312–325.
18. Bryson AE, Ho Y-C. *Applied Optimal Control*, chapter 3. Hemisphere: Washington, DC, 1975.
19. Athans M, Falb PL. *Optimal Control*: *An Introduction to the Theory and its Applications*. McGraw-Hill: New York, 1996; 288–289.

DOI: 10.1002/oca